Petroleum Research xxx (xxxx) xxx

Contents lists available at ScienceDirect

Petroleum Research

journal homepage: http://www.keaipublishing.com/en/journals/petroleum-research/

Insights into wettability alteration during low-salinity water flooding by capacitance-resistance model

Davood Zivar [a, b], Akzhol Ishanov [a], Peyman Pourafshary [a, *]

[a] School of Mining and Geosciences, Nazarbayev University, Nur-Sultan, Kazakhstan
[b] PanTerra Geoconsultants B.V, Leiderdorp, Netherlands

ARTICLE INFO

Article history:
Received 18 October 2021
Received in revised form
13 January 2022
Accepted 13 January 2022
Available online xxx

Keywords:
Wettability alteration
Capacitance-resistance model (CRM)
Time constant
Low salinity water
Data-driven

ABSTRACT

The capacitance-resistance model (CRM) has been widely implemented to model and optimise water-flooding and enhanced oil recovery (EOR) techniques. However, there is a gap in the application of CRM to analyse physical phenomena in porous media as well as the performance of EOR methods, such as low-salinity water (LSW) flooding. The main purposes of this study were to investigate how changes in time constant, as a CRM parameter, can represent physical phenomena in porous media such as wettability alteration. Moreover, to show CRM is a reliable tool to use for interpretation of LSW process as an EOR method. The results of different experimental/modelling studies in this research showed that in CRM model time constant increases when the wettability alters to a water wetness state, whereby the smallest time constant value is observed for the oil wet medium and the highest is observed for the water wet medium. The cases with a gradual alteration in wettability show an increasing trend with the dilution of the injection water. The core flooding data confirms the observed results of the simulation approach. The increment in time constant values indicates the resistance against displacing fluid, which is due to the wettability alteration of the porous medium, resulting in additional oil production. The observations made during this research illustrate that the time constant parameter can be a powerful tool for comparing different EOR techniques, since it is a good indication of the speed of impact of a particular injection fluid on production.

1. Introduction

A considerable amount of oil always remains in the reservoir after the primary and secondary stages of production (Khosravi et al., 2021; Lake et al., 1992; Surajudeen et al., 2019). To bring the remaining oil into the production stream, a tertiary stage of production needs to be employed using different methods of enhanced oil recovery (EOR). Therefore, prediction of the performance of EOR methods and the subsequent selection of the best method are essential.

Different EOR methods are used to increase the ultimate oil recovery from reservoirs, including gas injection, polymer injection, water alternative gas injection (WAG), thermal methods and low salinity water (LSW) injection. In particular, LSW injection is one of the most applicable and economical methods and does not require special surface facilities or complicated operational conditions. It has been reported that LSW works for sandstone and carbonate reservoir rocks at both laboratory (Lager et al., 2008) and field scales (Vledder et al., 2010). Moreover, the combination of LSW and other EOR methods, such as low-salinity surfactant flooding (Alagic and Skauge 2010; Zivar et al., 2021), low-salinity polymer flooding (Karimov et al., 2020) and low-salinity water alternative CO_2 injection (Moradpour et al., 2021), has shown promising performance. Since Martin (1959) first investigated the applicability of LSW injection (Martin 1959), the topic has been investigated by many researchers in order to study the active mechanisms, performance, applicability and required operating conditions. Based on the findings, the responsible mechanisms for additional oil recovery while using LSW are wettability alteration (Khosravi et al., 2020), multicomponent ion exchange (Al-Abri et al., 2019; Lager et al., 2008; Shabani and Zivar 2020), double-layer expansion (Lee et al., 2011; Mahani et al., 2015), emulsification (Mahzari and Sohrabi 2015; Moradpour et al., 2021), the effect of pH change (Austad et al., 2010; McGuire et al., 2005; Morrow and

* Corresponding author.
E-mail address: Peyman.Pourafshary@nu.edu.kz (P. Pourafshary).

https://doi.org/10.1016/j.ptlrs.2022.01.004

Please cite this article as: D. Zivar, A. Ishanov and P. Pourafshary, Insights into wettability alteration during low-salinity water flooding by capacitance-resistance model, Petroleum Research, https://doi.org/10.1016/j.ptlrs.2022.01.004

Buckley 2011), fines migration (Fouladi et al., 2019; Tang and Morrow 1999), osmosis pressure (Sandengen and Arntzen 2013) and mineral dissolution (Shabani and Zivar 2020).

There are several types of uncertainty during numerical modelling of LSW process which affect the final results due to large number of mechanisms involved. Hence, a simpler method compared to numerical modelling with less input data is required to simulate the performance of the LSW. Among the available methods, predictive models usually meet the time and economic restrictions due to their rapidity and inexpensiveness. Predictive models are simple models that use material balance equations to investigate reservoir characteristics and performance. One of these predictive approaches is known as the capacitance-resistance model (CRM), which is widely used in many fields (Dastgerdi et al., 2020; Sayarpour 2008; Shabani et al., 2020). Only injection and production data are required for history matching in this approach, which makes the process fast and low cost. As a result, it is possible to carry out a rapid assessment of reservoir characteristics and predict the performance of production wells without the use of a complex numerical reservoir simulator.

The CRM is based on the resemblance to the technique of signal processing. In this model, the injection rates are considered as input signals and the production rates are considered as the output signals, which are responses of the reservoir to the input signals. The CRM employs the concepts of interwell connectivity to compensate for the lost portion of the injected fluid that does not contribute to production. The historical records of injection/production rates can be utilised to identify the connectivity between injector and producer pairs (Sayarpour 2008). The CRM uses the law of conservation of mass and deliverability equation as a basis to predict the future production rate of wells. Different forms of the CRM, such as the CRM tank (CRMT), CRM producer (CRMP) and CRM injector-producer (CRMIP), are used in the petroleum industry based on the control volume (Shabani et al., 2020). We present the general equations of the CRM and refer to Yousef et al. (2006) and Sayarpour (2008) for detailed derivations of the CRM and its different forms (Sayarpour 2008; Yousef et al., 2006). The material balance equation for the flooded reservoir is given by:

$$c_t \cdot V_p \cdot \frac{d\overline{p}}{dt} = w(t) - q(t) \tag{1}$$

where c_t is the total compressibility of a porous medium saturated with fluids, V_p is the total volume of pores or void space, $\overline{p}$ is the volume averaged pressure of the reservoir, $w(t)$ is the volumetric rate of injection at time t and $q(t)$ is the volumetric rate of production at time t.

The deliverability equation of a well (Alarifi et al., 2015) is written as:

$$q_t = J \cdot \left(\overline{p}(t) - p_{wf}(t)\right) \tag{2}$$

where $\overline{p}(t)$ is the volume averaged pressure of the reservoir at time t, $p_{wf}(t)$ is the bottom hole pressure (BHP) of the producer at time t and J is the productivity index.

Expressing $\overline{p}(t)$ from Eq. (2) and substituting into Eq. (1) results in:

$$\tau \cdot \frac{dq}{dt} + q(t) = w(t) - \tau \cdot J \cdot \frac{dp_{wf}}{dt} \tag{3}$$

where τ stands for the time constant and is expressed by:

$$\tau = \frac{c_t \cdot V_p}{J} \tag{4}$$

Finally, by considering the stepwise alteration of injection flowrates and linear changes of BHP at every time step Δt_k, the analytical solution to Eq. (3) can be written as Eq. (5).

$$q(t_n) = q(t_0) \cdot e^{-\frac{t_n - t_0}{\tau}} + \sum_{k=1}^{n} \left(\left(1 - e^{-\frac{\Delta t_k}{\tau}}\right) \cdot \left(w(t_k) - J \cdot \tau \cdot \frac{\Delta p_{wf}(t_k)}{\Delta t_k} \right) \cdot e^{-\frac{t_n - t_k}{\tau}} \right) \tag{5}$$

The above equation suggests that $q(t)$, as the output signal, can be decomposed into a) the response of the initial production rate, b) the response of the input signal (injection) and c) the response of the output signal (considering BHP variations). The final form of the CRM for multiple injection and production wells and at constant BHP is presented as:

$$q_j(t_k) = q_j(t_k - 1) e^{-\frac{\Delta t_k}{\tau_j}} + \left(1 - e^{-\frac{\Delta t_k}{\tau_j}}\right) \sum_{i=1}^{n_i} f_{ij} w_i(t_k) \tag{6}$$

where the interwell connectivity (f_{ij}) is a parameter of the CRM that indicates to what extent the injected water from a specific injector (i) affects the total production from a specific producer (j).

In analysing the CRM, the interwell connectivity and time constant play important roles. Interwell connectivity is crucial in the management of secondary and tertiary production, as it provides knowledge regarding the reservoir's behaviour and the response to injection variables. The time constant is a parameter that considers the dissipation of input signals in formation rock. As described previously, in the CRM, the inputs are injection rates and the BHPs of producers, which change with time. During primary recovery, the time constant is also associated with the production decline. The time constant can be expressed by Eq. (4). The evaluation of Eq. (4) indicates that a large pore volume or/and a highly compressible system with a low productivity index lead to the high value of the time constant, which results in a significant delay to the response to the input signals. In contrast, the fast input signal transition and the rapid decline of the primary recovery term results from the low value of the time constant.

Although the CRM was developed for water flooding, it has been used for the evaluation of different EOR methods. Considering the fact that any EOR method deals with a complicated interaction between fluids and rock, history matching and predicting such a process is possible using a simple CRM approach. Table 1 summarises the studies conducted in this area.

The presented studies in Table 1 are proof of the progress made in using the CRM for the waterflooding process and analysing different EOR methods using CRM. However, the effect of initial wettability and wettability alteration by LSW flooding, as an EOR method, on the CRM parameters has not yet been studied. Moreover, there is no available literature to use CRM in interpreting core flooding data. Therefore, in this study, the main objectives are to evaluate the ability of the CRM to interpret the wettability

Table 1
Application of CRM to EOR processes.

EOR method	Highlights	Reference
CO_2 flooding	An equation was proposed to predict the enhancement in oil rate due to the injection of CO_2 while the CO_2 injection rate was considered constant. The proposed solution requires the history matching of four parameters for the injection gas.	Sayarpour (2008)
	A semi-empirical power-law fractional flow model in conjunction with the CRMP was used to optimise a miscible CO_2 flooding process.	Eshraghi et al. (2016)
WAG	WAG injection into the McElroy field, Permian Basin, West Texas was investigated using CRMP and CRMT approaches with the semi-empirical power-law fractional flow model.	Sayarpour (2008)
Simultaneous water and gas (SWAG)	An oil rate model was derived to deal with water and CO_2 separately while both of them pushing oil to the injectors with known relative permeability curves.	Nguyen (2012)
Gas injection	The CRM was modified based on gas density and average reservoir pressure. The modified model was also coupled with a genetic algorithm. The obtained results in comparison with streamline simulation showed reliable interwell connectivity and oil rate prediction.	Yousefi et al. (2019)

alteration as a physical phenomenon encountered in porous media and to investigate the application of the CRM in LSW flooding as an EOR method.

In this study, two approaches are used to satisfy the objectives. First, several scenarios are simulated by CMG-GEM to generate injection/production histories for the media with different initial wettabilities, as well as the wettability alteration by LSW injection. Then, the CRM approach is used to extract the time constant values for the different simulation scenarios. Second, the data of two core samples that were under LSW flooding are used to compare with the obtained results from the simulation section and validate the observed results. In the final step, it is shown that time constant (as a CRM parameter) is able to predict physical phenomena such as wettability alteration. Moreover, CRM is reliable tool to use for interpretation of the LSW process as an EOR method.

2. Methodology

To analyse the effect of different wettability conditions and the alteration of wettability due to the injection of LSW on the time constant (as a CRM parameter), two main approaches were used. First, the time constant was estimated by a series of simulation models. In the first step of the simulation approach, three porous media with initial wettabilities of water wet (WW), mixed wet (MW) and oil wet (OW) were flooded with water. In the second step of the simulation approach, three porous media with the same properties were flooded with three different LSWs (Caspian Sea water (CSW) and 5 × and 10 × diluted waters). Second, the data of two core samples with initial wettabilities of OW and WW, which were under LSW, were used to validate the simulation approach. The obtained histories of injections and productions were then used to calculate time constant values using the CRM approach. Fig. 1 shows the workflow of this study.

2.1. Simulation models and properties

To study the time constant, the injection/production history at different wettability conditions and salinities of the water is required. Hence, a model was developed to generate the injection and production histories. The model was developed in CMG-GEM with dimensions of 30 (i) × 1 (j) × 1 (k) grid blocks. The length of the grid blocks in the i and j directions are equal to 150 ft and in the k direction is equal to 10 ft. It should be mentioned that this study deals with one-dimensional models in order to eliminate the effect of interwell connectivity (f_{ij}) and focus on the time constant (τ). Moreover, the similarity between one-dimensional simulation models and core flooding in terms of the direction of fluids flow makes the comparison and validation possible. One injector and one producer contribute to the model, as shown in Fig. 2. The detailed properties of the model are presented in Table 2. Heptane

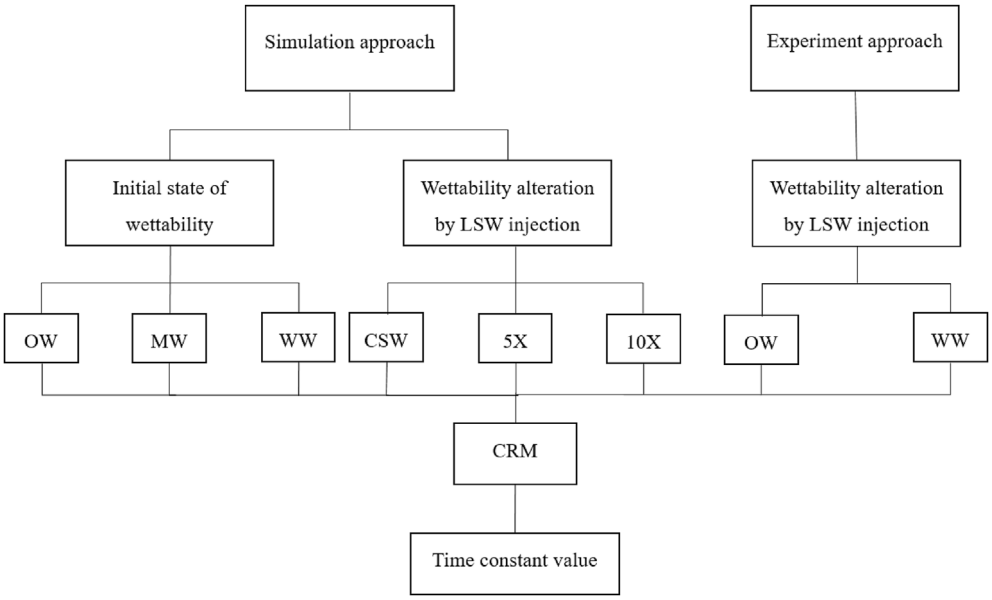

Fig. 1. Workflow diagram of this study.

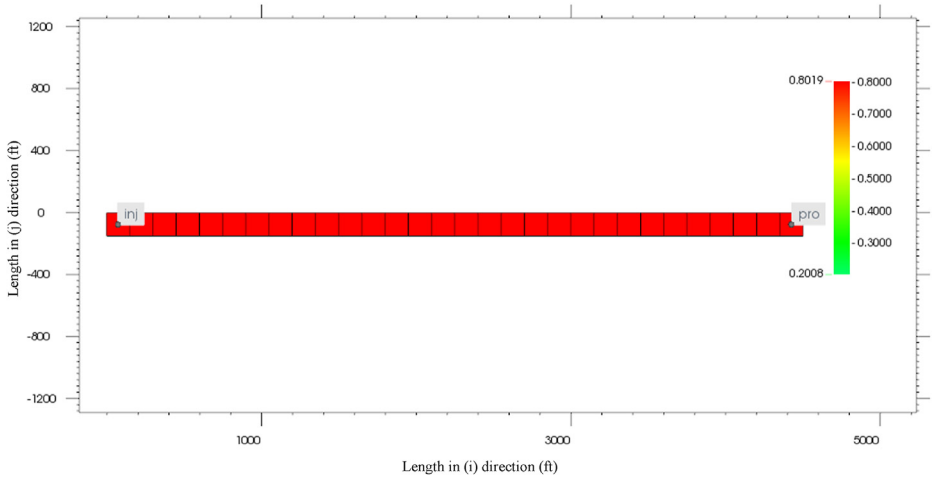

Fig. 2. Geometry of the model (color bar shows saturation of the oil).

Table 2
Properties of the simulation model.

Properties	Value
Porosity	20%
Permeability	100 mD
Initial reservoir pressure	3000 psi
Initial water saturation	0.2
Rock compressibility	2×10^{-10} 1/psi
Simulation duration	2191 d (6 years)

(C_7H_{16}) is used as the contributing hydrocarbon component in the model to reduce complexity.

A sensitivity analysis was conducted on the number of grid blocks to determine the appropriate grid block number to avoid numerical error and unreliable results (see Fig. 3). This analysis was carried out on two parameters simultaneously, namely, the breakthrough time (BT) and the cumulative fluid produced during the simulation, as they are important parameters that are used in CRM analysis. The results show that there is a significant difference between the BT and cumulative fluid for the model with 15 and 30 grid blocks. The difference between 30 and 45 grid blocks is ignorable; thus, the model with 30 grid blocks was chosen for further analysis to reduce computational costs. It should be mentioned that normal variation in pressure, saturation and global composition per timestep reduce in all simulation scenarios in order to avoid numerical dispersion.

To investigate the effect of different states of wettability and wettability alteration on the time constant, three porous media with different initial wettabilities (WW, MW and OW) were used to generate the 6-year injection/production history. The different wettabilities were dictated in the simulation using different relative permeability curves. The models were then flooded with water based on the pre-defined schedule. In the second scenario, the wettability is gradually changed from the OW state to the WW condition due to the alteration in the concentration of ions in the water. This concept is based on gradually wettability alteration of the porous media when it is under LSW flooding (Negahdari et al., 2021). We assumed that the reservoir rock properties, such as porosity, compressibility and absolute permeability, remained the same for all the scenarios.

The oil and water relative permeability values depend on the wettability of rock (Khosravi 2012). Therefore, the corresponding relative permeability data should be introduced for the OW and

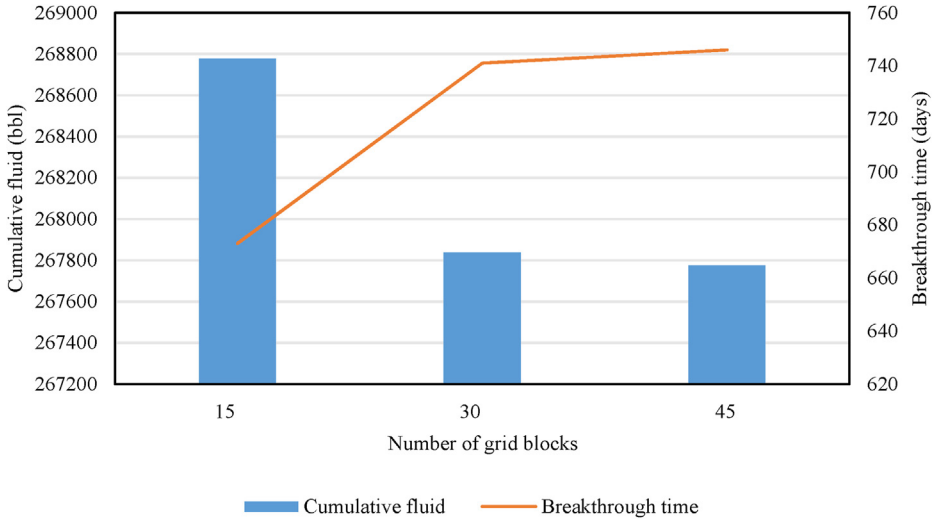

Fig. 3. Sensitivity analysis of the number of grid blocks.

Table 3
Criteria for assessing rock wettability.

Criteria	OW	WW	Reference
End-point relative permeability to oil at S_{wi}	<0.70–0.80	>0.95	Owens and Archer (1971)
End-point relative permeability to water at S_{or}	>0.50	<0.30	Craig (1971)
Initial water saturation, S_{wi}	<0.15	>0.20	Craig (1971)
Water saturation at cross-over point	<0.50	>0.50	Craig (1971)

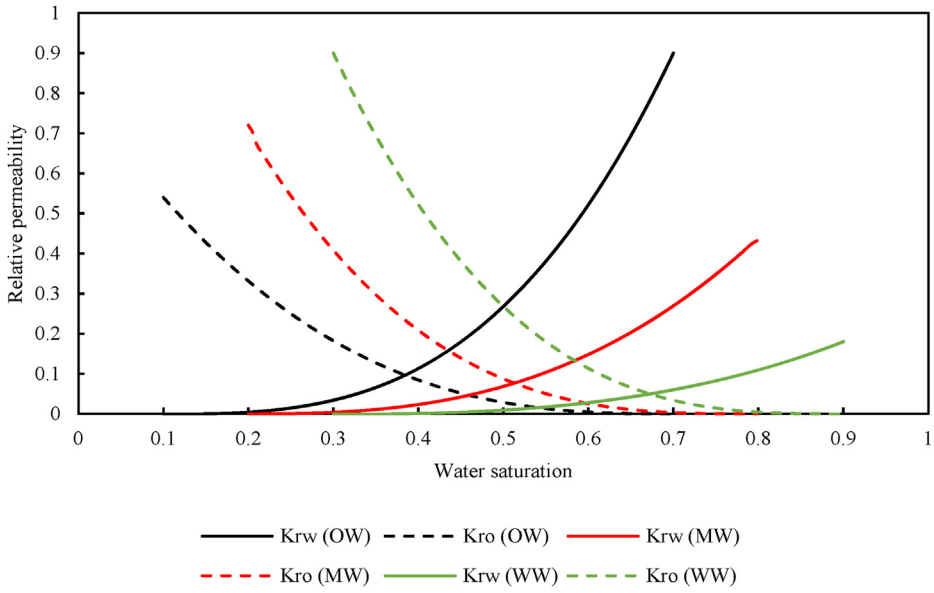

Fig. 4. Water/oil relative permeability curves for OW, MW and WW systems.

WW systems. The rule of thumb proposed by Owens and Archer (1971) and Craig (1971) was implemented to generate truthful relative permeability data for the OW and WW states of wettability (Craig 1971; Owens and Archer 1971). The criteria are given in Table 3.

The developed relative permeability curves for the OW, MW and WW systems by interpolation are demonstrated in Fig. 4.

The CSW and 5 × and 10 × diluted water are considered as injecting fluids in the third scenario, as presented in Table 4. The formation brine used in this study is representative of the oil field in West Kazakhstan. CSW was used as LSW, the composition of which was measured by Metrohm 930 Compact IC Flex ion chromatographer. Other LSW samples were prepared by diluting CSW. Ion concentrations were calculated based on the stoichiometry and molecular mass of the compounds (Bazhanova and Pourafshary 2020).

The geochemical reactions that contribute to the simulation models are described as Eqs. (7) through (11).

$$OH^- + H^+ \leftrightarrow H_2O \tag{7}$$

$$Ca^{2+} + SO_4^{2-} \leftrightarrow CaSO_4 \tag{8}$$

$$Mg^{2+} + SO_4^{2-} \leftrightarrow MgSO_4 \tag{9}$$

$$H^+ + SO_4^{2-} \leftrightarrow HSO_4^- \tag{10}$$

$$HCO_3^-(aq) + Ca^{2+}(aq) \leftrightarrow CaCO_3(s) + H^+(aq) \tag{11}$$

When wettability alteration takes place as a result of the LSW injection, the oil/water relative permeability also changes, which can be captured using interpolation between the relative permeability curves based on the concentration of active ions, such as SO_4^{2-} (λ). A weighting factor (ω) is used to show the relative permeability alteration as Eq. (12).

$$\omega = \frac{\lambda - \lambda^{HSW}}{\lambda^{LSW} - \lambda^{HSW}} \tag{12}$$

where λ is the overall concentration of SO_4^{2-}, λ^{HSW} is the concentration of SO_4^{2-} in the HSW (here HSW is formation brine) and λ^{LSW}

Table 4
Composition of LSW streams.

	Cl^-	SO_4^{2-}	Na^+	K^+	Ca^{2+}	Mg^{2+}	TDS (ppm)
Formation water	104,980	N/A	54,500	N/A	9450	1450	170,380
Caspian Sea water (CSW)	7215	3145	4975	155	535	770	16,795
5 × dilution	1443	629	995	31	107	154	3359
10 × dilution	722	315	498	16	54	77	1682

is the overall concentration of SO_4^{2-} in the LSW. The water and oil relative permeability values are calculated by Eqs. (13) and (14)

$$K_{rw} = \omega K_{rw}^{LSW} + (1-\omega) K_{rw}^{HSW} \tag{13}$$

$$K_{ro} = \omega K_{ro}^{LSW} + (1-\omega) K_{ro}^{HSW} \tag{14}$$

where K_{rw} is the calculated water relative permeability, K_{ro} is the calculated oil relative permeability, K_{rw}^{LSW} is the water relative permeability (LSW injection), K_{rw}^{HSW} is the water relative permeability (HSW injection), K_{ro}^{LSW} is the oil relative permeability (LSW injection) and K_{ro}^{HSW} is the oil relative permeability (HSW injection). Fig. 5 demonstrates the injection scheme during the simulation time for all scenarios.

2.2. Core flooding data

The injection and production history of two carbonate core flooding experiments were used to study the effect of LSW flooding on the CRM parameters. The effect was analysed for different initial wettability states. To achieve this, the data obtained by the core flooding experiments conducted by Shakeel et al. (2021a, 2021b) was used in this study, as shown in Table 5.

In all tests, the HSW was injected, followed by LSW flooding. The mineralogy and types of cores were the same but the wettability of the cores was different due to the different aging periods by oil. Two cores were selected to represent the OW (sample no. 1) and WW (sample no. 2) states. The oil used in the core flooding experiment had a viscosity of 10.8 cp and a density of 0.868 g/cc. All core flooding cases were performed under a back pressure of 500 psi and a temperature of 80 °C. First, the HSW injection was performed on the core samples at injection rates of 0.5, 2.0 and 5.0 cc/min. LSW injection was then performed at the same injection rates. Fig. 6 presents the injection scheme for both core samples.

2.3. History matching by CRM

The CRM is able to predict the rate of the producer(s) using Eq. (6). In our calculations, the time interval (Δt) was considered to be equal to 1 month. The history matching process was conducted based on the objective function (Eq. (15)). As the simulation model used in this study consists of one injector and one producer, the interwell connectivity (f_{ij}) is equal to 1.

$$minq = \sum_{k=1}^{n_t} \left(q_{obs} - q_{pre}\right)^2 \tag{15}$$

where *minq* is the objective function, which should be minimised, k is the number of time intervals, n_t is the total number of time intervals, q_{obs} is the observed flow rate and q_{pre} is the predicted flow rate. The final estimation of the time constant was obtained by fitting the injection/production histories based on the physical constraints and objective function.

3. Results and discussion

3.1. Time constant from simulation models

3.1.1. Different states of wettability

The history matching of the observed and estimated total production rates for different states of initial wettability was performed by the CRM (see Fig. a1 of the Appendix). The results show that the CRM is able to predict the simulated rates with a high level of confidence. Fig. 7 presents the estimated time constants for the OW, MW and WW media. As shown in this figure, the time constant increases when the wettability of the porous medium changes from OW to WW.

It is believed that the flow resistance of the non-wetting phase decreases as the wettability of the porous media to the wetting phase increases. Here, water, as the non-wetting phase in the OW medium, finds its way to the production well faster compared to the MW and WW systems. This has been confirmed experimentally and numerically in the literature (Anderson 1987; Li et al., 2005; Zhao et al. 2017, 2018). We also show this phenomenon by presenting the values of the water velocity in the 29th block in the (i) direction, which are equal to 0.306, 0.258 and 0.202 ft/day for the OW, MW, and WW systems, respectively (see Table 6). In addition, we used water cuts as a sign to show how fast the signal would be received by the producer. The water cuts for the OW, MW and WW systems are illustrated in Fig. 8. As shown, the water cut starts to increase at 737, 976 and 1090 d in the OW, MW and WW systems, respectively (see Table 6). Thus, it can be inferred that when the injecting fluid

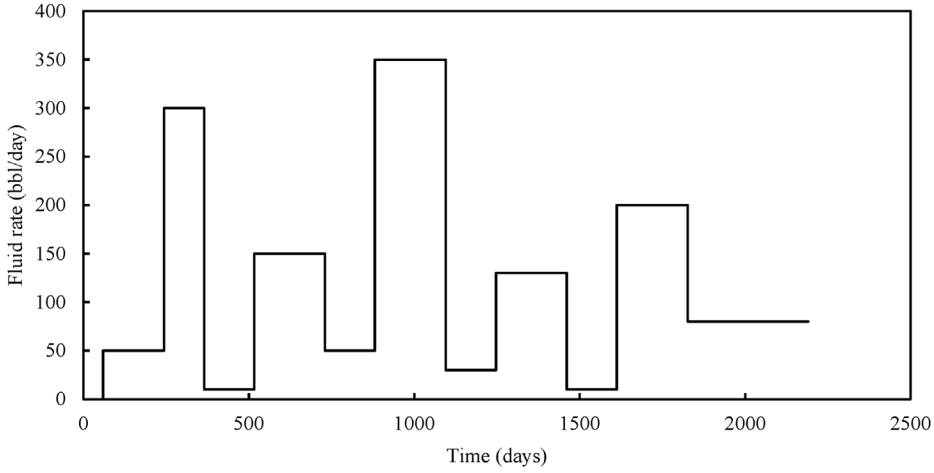

Fig. 5. Injection scheme used in the simulation model.

Table 5
Parameters of core samples.

Sample number	Initial state of wettability	Porosity (%)	Permeability (md)	Ultimate recovery factor (%)
1	OW	14.60	103.6	52.3
2	WW	14.83	134.4	76.0

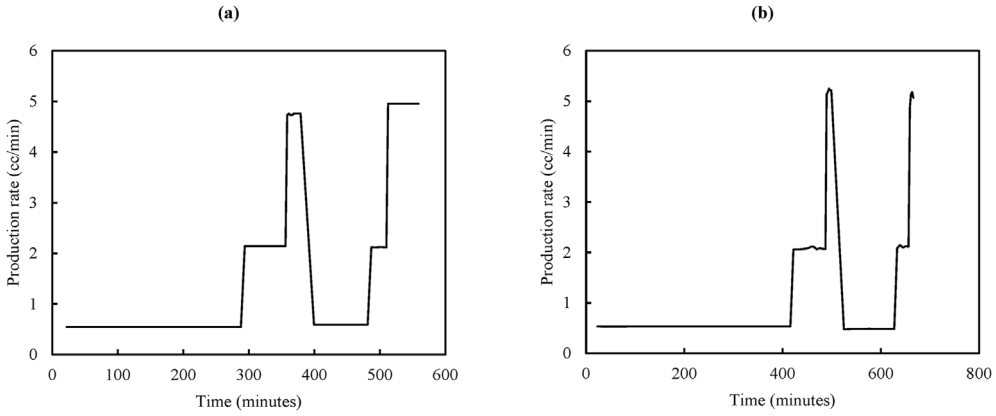

Fig. 6. Injection scheme for (a) OW and (b) WW.

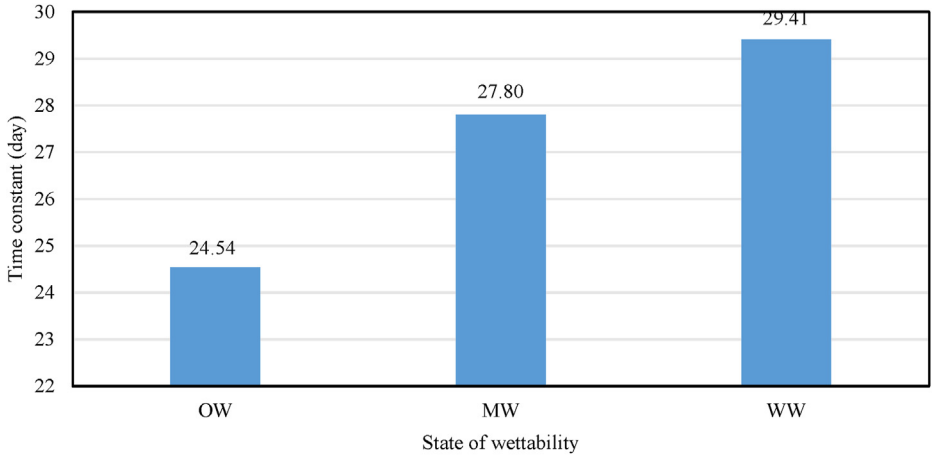

Fig. 7. Time constants for different states of initial wettability.

Table 6
Selected parameters from the simulation models.

	OW	MW	WW	CSW	5×	10×
Water velocity (ft/day) @ block (29, 1, 1)	0.306	0.258	0.202	0.260	0.254	0.251
Average pressure (psi) @ block (29, 1, 1)	1312	1360	1504	1421	1430	1435
Average oil flux (bbl/day) @ block (29, 1, 1)	38.9	49.4	63.2	50.5	52.2	53.0
BT (d)	737	976	1090	791	797	798
Ultimate recovery factor (%)	48.19	62.54	79.73	61.62	63.64	64.56

shows less resistance, the response can be seen in the producer sooner, resulting in a smaller time constant. This was also noted by Yousef et al. (2006), where a nearly instantaneous and equal change can be seen in the producer when the time constant is small (Yousef et al., 2006). The results of this scenario obviously demonstrate the time constant to be a reliable parameter that can indicate the wettability of porous media.

3.1.2. Wettability alteration from LSW injection

The production rates during the injection of LSW with different salinities were history matched by the CRM using the injection/production data obtained during the simulation. The predicted production rates are in good agreement with the observed values (see Fig. a2 of the Appendix), which shows the applicability of the CRM for predicting the EOR process by LSW injection. Fig. 9 presents the time constants for the process of LSW injection with

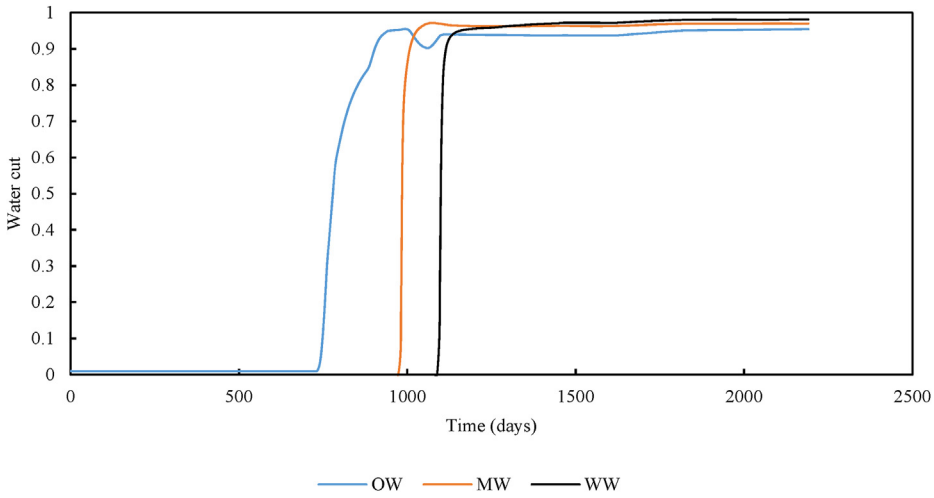

Fig. 8. Water cut for different states of initial wettability.

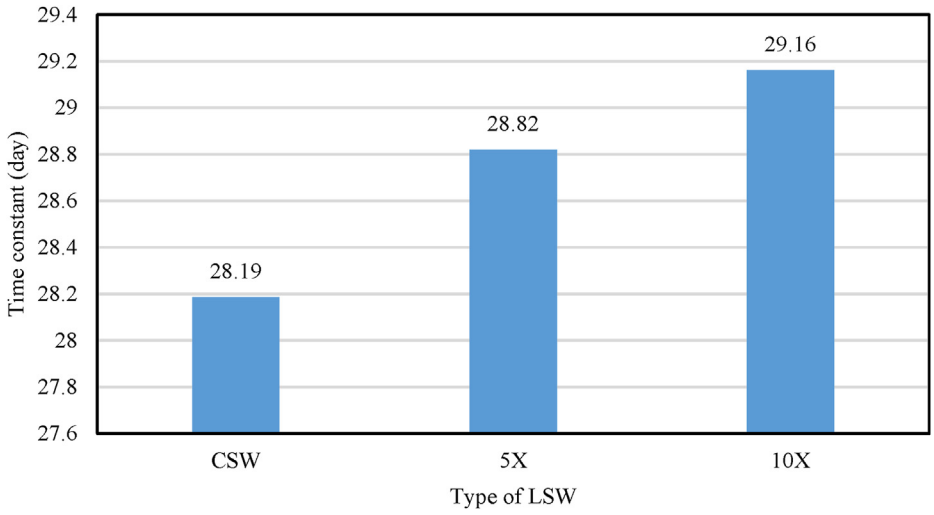

Fig. 9. Time constants for different salinities of injected water.

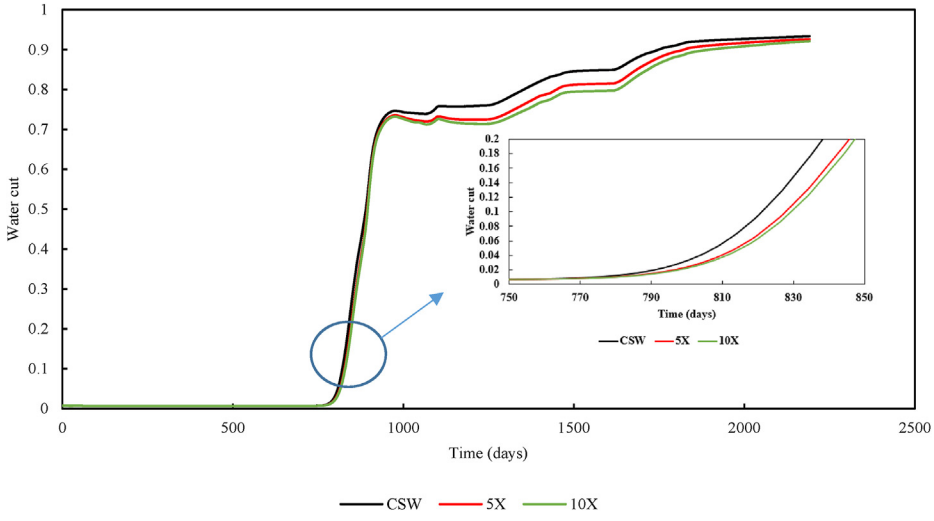

Fig. 10. Water cut for different salinities of injected water.

different salinities. As can be seen in this figure, the time constant increases when the salinity of the injected water decreases.

The BTs are in the narrow range of 791–798 d but the trend of increasing is different, where the CSW with a higher salinity shows a sharper increasing trend compared to the 5 × and 10 × diluted waters (Fig. 10). The water cut of the 5 × diluted water is slightly higher than the 10 × diluted water. This observation is in line with the results of Bazhanova and Pourafshary (2020) in the core scale, where 5 × diluted water was selected as the optimised LSW sample (Bazhanova and Pourafshary 2020).

The time constants of this scenario show a range of 28.19–29.16 and are between the initial wettabilities of MW (27.8) and WW (29.41). The average water velocity at the 29th grid block is similar to MW and the BT is between the OW and MW media ($702 < 791–798 < 967$) for all three cases of this scenario. The magnitude of the ultimate recovery factors is similar (±2% difference) to the ultimate recovery factor of the MW medium (62.54%). From the obtained results, it can be inferred that the overall state of wettability during the LSW flooding (gradual alteration of wettability) is placed between MW and WW. It is also showed that although the BT occurs faster compared to the MW medium, the ultimate performance of the process increases when the wettability gradually changes. The results of this scenario highlight two important points. First, the time constant can be representative of the wettability alteration during LSW injection. Second, gradual alteration of the wettability improves the ultimate performance of the process.

3.2. Time constant from core flooding data

The total production rates are history matched by the CRM for OW and WW conditions using the injection data recorded during core flooding tests. The observed and modelled production rates show good agreement (see Fig. a3 of the Appendix), illustrating that the CRM is capable of predicting the results of the experiments with good accuracy. Fig. 11 presents the time constants for flooding of the OW and WW core samples with LSW. As can be seen in this figure, the time constant is smaller in the case of the OW core sample compared to the WW core sample.

The same trend was observed for the time constants in the core flooding experiments. In addition, the BTs confirm this observation when the water finds a way to the production stream after 14 and 17 min for the OW and WW core samples, respectively. The results of this section illustrate that the alteration of wettability affects the time constant and also validate the simulation results.

4. Do changes in the time constant represent wettability alteration?

The findings show time constant is good representative of wettability alteration in the porous media. The time constant, as one of the key parameters of the CRM, is representative of the porous media response to the input signal. The changes in the time constant depend on the reservoir rock and fluid properties, as well as the operating conditions. For example, the production well can sense the input signal faster if the signal fly path is facilitated, resulting in a reduction in the value of the time constant, or a porous medium filled with incompressible fluid shows a smaller time constant compared to the same porous medium with a compressible fluid. Therefore, the time constant is able to present physical phenomena in the porous media.

During the EOR with LSW injection, several mechanisms may happen simultaneously based on the rock and fluid interactions, which finally lead to additional oil recovery. The most possible and well-known scenario is wettability alteration due to the injection of water with lower salinity or the injection of an ion-engineered water. The injection of such water causes changes in the fluid flowability (relative permeability and capillary pressure curves) and the distribution of the fluids in the porous media (such as the pull and push mechanism and the redistribution of fluids). It is believed that switching to LSW removes the barriers against additional oil production. Thus, LSW injection brings more oil into the production stream by facilitating the flow of oil.

The results of this study show that the time constants of the CRM increase when the wettability of the medium alters toward a more WW state. Such an increment in the time constant is due to the fact that the interactions between the rock and fluids increase because more volume of oil is available to displace by displacing

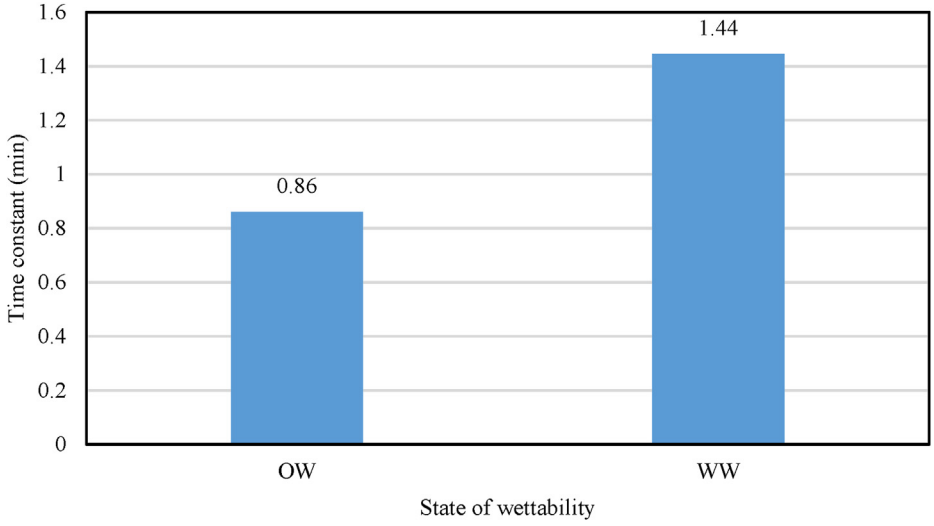

Fig. 11. Time constants for core flooding experiments.

fluid (water), resulting in higher resistivity against flowing water as a signal sent from an injector to a producer. In other words, the observed increment in time constants shows that the wettability of the porous medium is changed to a state where there are less conductive paths for flowing water.

5. Conclusions

This study investigated the effect of different initial wettabilities and wettability alteration by LSW flooding on the time constant as a CRM parameter. Several scenarios were simulated by CMG-GEM to generate injection/production histories. Moreover, the core flooding data were used to validate the hypothesis. The producer-based CRM was then used to estimate time constants for different scenarios. The obtained results from the different scenarios have shown that:

- Changes in wettability, either by injecting LSW or different initial wettabilities, affect the time constant of the CRM.
- The time constants logically present the state of wettability and wettability alteration of porous media.
- The time constants show an increasing trend when the wettability of the porous media alter from oil wet to mixed wet and from mixed wet to water wet.
- The results of core flooding confirm the observed trend in the simulation approach.
- Changing the state of wettability after a period of production causes the overall magnitude of the time constant to increase, which means a favourable state of wettability.
- Changing the state of wettability by a stepwise manner increase results in time constants close to water wet, which is representative of the improvement in the performance of the process.

Declaration of competing interest

We confirm that there is no conflict of interest in our submitted publication and our research.

Acknowledgment

The authors would like to thank Nazarbayev University for supporting this research through the NU Faculty Development Competitive Research Grants program (Award number: 110119FD4541).

Appendix

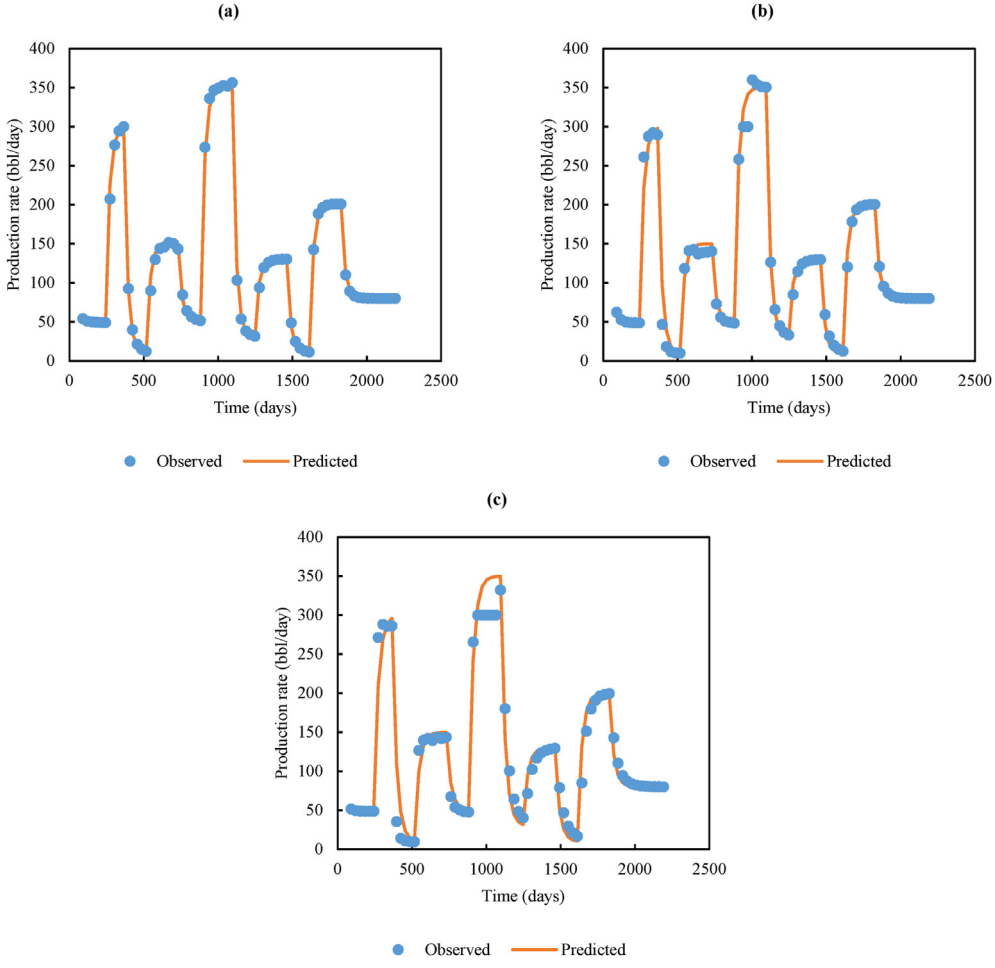

Fig.a1. Fluid (water + oil) production rates for different states of wettability: (a) OW, (b) MW, and (c) WW

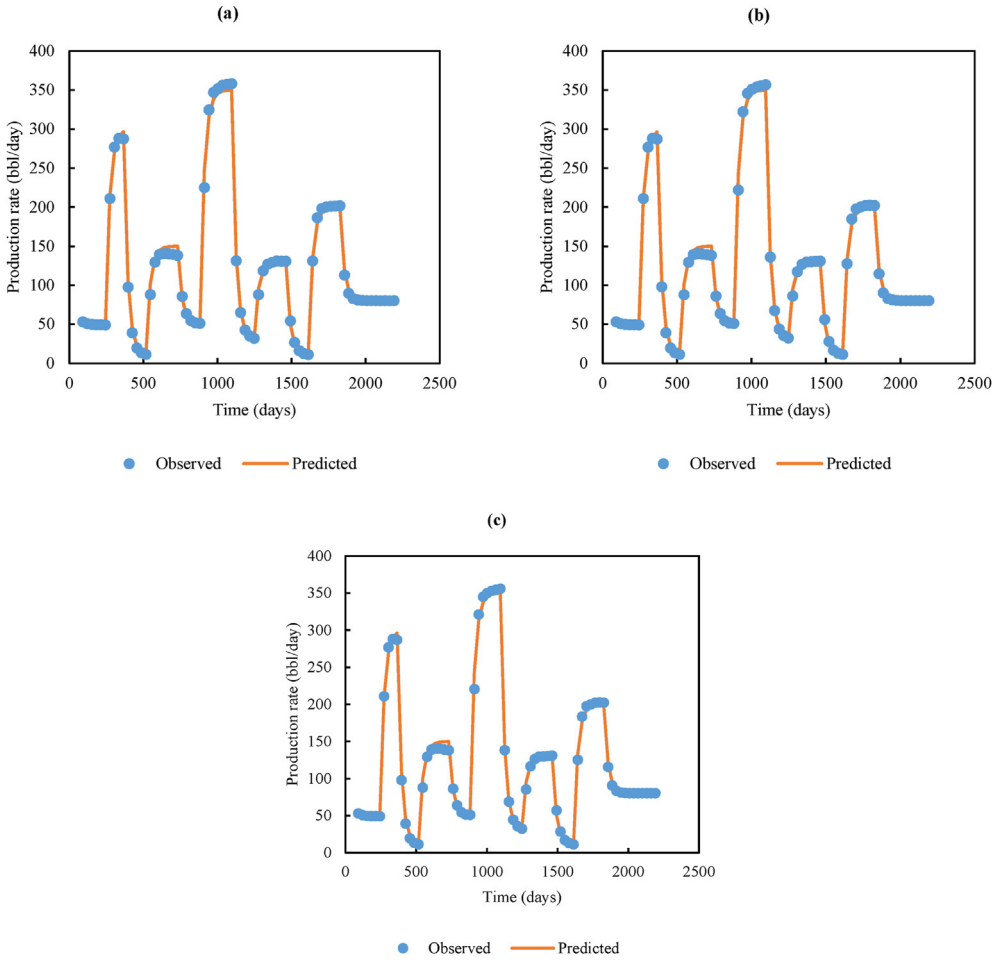

Fig.a2. Fluid (water + oil) production rates for different salinities of water: (a) CSW, (b) 5× dilution, and (c) 10× dilution

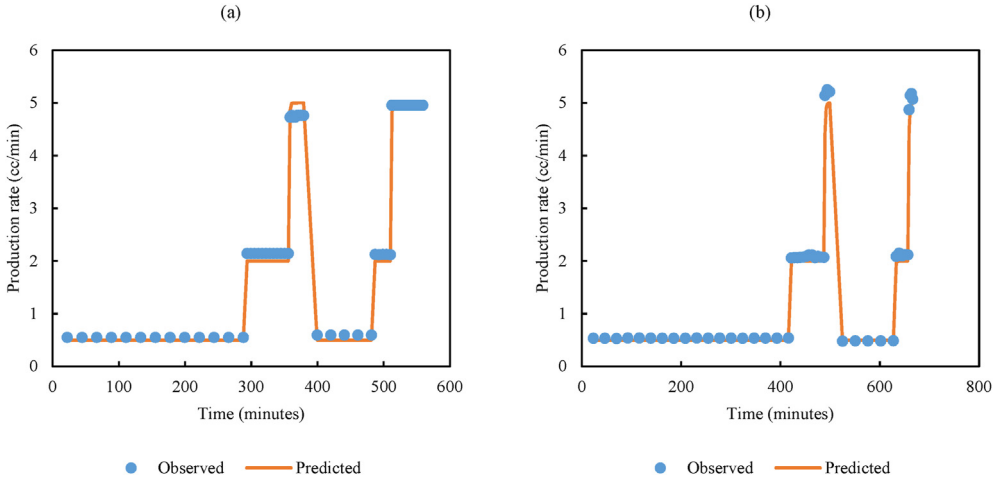

Fig.a3. Fluid (water + oil) production rates for core flooding experiments: (a) OW and (b) WW

References

Al-Abri, H., Pourafshary, P., Mosavat, N., Al Hadhrami, H., 2019. A study of the performance of the LSWA CO2 EOR technique on improvement of oil recovery in sandstones. Petroleum 5, 58–66. https://doi.org/10.1016/j.petlm.2018.07.003.

Alagic, E., Skauge, A., 2010. Combined low salinity brine injection and surfactant flooding in Mixed–Wet sandstone cores. Energy Fuel. 24, 3551–3559. https://doi.org/10.1021/ef1000908.

Alarifi, S., AlNuaim, S., Abdulraheem, A., 2015. Productivity index prediction for oil horizontal wells using different artificial intelligence techniques. In: Paper Presented at the SPE Middle East Oil & Gas Show and Conference. https://doi.org/10.2118/172729-MS.

Anderson, W.G., 1987. Wettability literature survey Part 5: the effects of wettability on relative permeability. SPE-129421-JPT. 39, 1453–1468. https://doi.org/10.2118/16323-PA.

Austad, T., Rezaeidoust, A., Puntervold, T., 2010. Chemical mechanism of low salinity water flooding in sandstone reservoirs. In: Paper Presented at the SPE Improved Oil Recovery Symposium, Tulsa, Oklahoma, USA, 2010/1/1/. https://doi.org/10.2118/129767-MS.

Bazhanova, M., Pourafshary, P., 2020. Impact of SO42−, Ca2+, and Mg2+ ions in Caspian Sea ion-engineered water on the rate of wettability alteration in carbonates. Journal of Petroleum Exploration and Production Technology 10, 3281–3293. https://doi.org/10.1007/s13202-020-01006-z.

Craig, F.F., 1971. The Reservoir Engineering Aspects of Waterflooding, 3. HL Doherty Memorial Fund of AIME, New York.

Dastgerdi, E.J., Shabani, A., Zivar, D., Jahangiri, H.R., 2020. Estimation of underground interwell connectivity: a data-driven technology. J. Taiwan Inst. Chem. Eng. 116, 144–152. https://doi.org/10.1016/j.jtice.2020.11.008.

Eshraghi, S.E., Rasaei, M.R., Zendehboudi, S., 2016. Optimization of miscible CO2 EOR and storage using heuristic methods combined with capacitance/resistance and Gentil fractional flow models. J. Nat. Gas Sci. Eng. 32, 304–318. https://doi.org/10.1016/j.jngse.2016.04.012.

Fouladi, M.M., Rostami, B., Pourafshari, P., 2019. Effects of the presence of fines on the performance of low salinity waterflooding. Spec. Top Rev. Porous Media Int. J. 10, 155–169. https://doi.org/10.1615/SpecialTopicsRevPorousMedia.2018025914.

Karimov, D., Hashmet, M.R., Pourafshary, P., 2020. A Laboratory Study to Optimize Ion Composition for the Hybrid Low Salinity Water/Polymer Flooding. https://doi.org/10.4043/30136-MS.

Khosravi, V., 2012. Various methods to detemine relative permeability in fractured reservoirs. In: Paper Presented at the SPE Asia Pacific Oil and Gas Conference and Exhibition. https://doi.org/10.2118/158384-MS.

Khosravi, V., Mahmood, S.M., Zivar, D., Sharifigaliuk, H., 2020. Investigating the applicability of molecular dynamics simulation for estimating the wettability of sandstone hydrocarbon formations. ACS Omega 5, 22852–22860. https://doi.org/10.1021/acsomega.0c02133.

Khosravi, V., Mahmood, S.M., Hosseini, S.J., Rostami, A., 2021. An atomistic investigation into water adsorption behavior on the surfaces of quartz (001) and calcite (001). Mater. Werkst. 52, 1073–1079. https://doi.org/10.1002/mawe.202000313.

Lager, A., Webb, K.J., Black, C.J.J., Singleton, M., Sorbie, K.S., 2008. Low salinity oil recovery - an experimental investigation. Petrophysics 49, 28–35.

Lake, L.W., Schmidt, R.L., Venuto, P.B., 1992. A Niche for Enhanced Oil Recovery in the 1990s.

Lee, S.Y., Webb, K.J., Collins, I.R., Lager, A., Clarke, S.M., Routh, A.F., O'Sullivan, M., 2011. Low Salinity Oil Recovery – Increasing Understanding of the Underlying Mechanisms of Double Layer Expansion. https://doi.org/10.3997/2214-4609.201404799.

Li, H., Pan, C., Miller, C.T., 2005. Pore-scale investigation of viscous coupling effects for two-phase flow in porous media. Phys. Rev. 72, 026705. https://doi.org/10.1103/PhysRevE.72.026705.

Mahani, H., Keya, A.L., Berg, S., Bartels, W.-B., Nasralla, R., Rossen, W.R., 2015. Insights into the mechanism of wettability alteration by low-salinity flooding (LSF) in carbonates. Energy Fuel. 29, 1352–1367. https://doi.org/10.1021/ef5023847.

Mahzari, P., Sohrabi, M., 2015. Impact of micro-dispersion formation on effectiveness of low salinity waterflooding. In: Paper Presented at the IOR 2015 - 18th European Symposium on Improved Oil Recovery. https://doi.org/10.3997/2214-4609.201412103.

Martin, J.C., 1959. The effects of clay on the displacement of heavy oil by water. In: Paper Presented at the Venezuelan Annual Meeting, Caracas, Venezuela, 1959/1/1/. https://doi.org/10.2118/1411-G.

McGuire, P.L., Chatham, J.R., Paskvan, F.K., Sommer, D.M., Carini, F.H., 2005. Low salinity oil recovery: an exciting new EOR opportunity for Alaska's north slope. In: Paper Presented at the SPE Western Regional Meeting, Irvine, California, 2005/1/1/. https://doi.org/10.2118/93903-MS.

Moradpour, N., Pourafshary, P., Zivar, D., 2021. Experimental analysis of hybrid low salinity water alternating gas injection and the underlying mechanisms in carbonates. J. Petrol. Sci. Eng. 202, 108562. https://doi.org/10.1016/j.petrol.2021.108562.

Morrow, N., Buckley, J., 2011. Improved oil recovery by low-salinity waterflooding. SPE-129421-JPT 63, 106–112. https://doi.org/10.2118/129421-JPT.

Negahdari, Z., Malayeri, M.R., Ghaedi, M., Khandoozi, S., Riazi, M., 2021. Gradual or instantaneous wettability alteration during simulation of low-salinity water flooding in carbonate reservoirs. Nat. Resour. Res. 30, 495–517. https://doi.org/10.1007/s11053-020-09726-z.

Nguyen, A.P., 2012. Capacitance Resistance Modeling for Primary Recovery, Waterflood and water-CO_2 Flood. University of Texas, Austin, TX, USA.

Owens, W.W., Archer, D.L., 1971. The effect of rock wettability on oil-water relative permeability relationships. SPE-129421-JPT. 23, 873–878. https://doi.org/10.2118/3034-PA.

Sandengen, K., Arntzen, O.J., 2013. Osmosis during Low Salinity Water Flooding. https://doi.org/10.3997/2214-4609.20142608.

Sayarpour, M., 2008. Development and Application of Capacitance-Resistive Models to water/CO_2 Floods. The University of Texas at Austin.

Shabani, A., Zivar, D., 2020. Detailed analysis of the brine-rock interactions during low salinity water injection by a coupled geochemical-transport model. Chem. Geol. 537, 119484. https://doi.org/10.1016/j.chemgeo.2020.119484.

Shabani, A., Moosavi, M.S., Zivar, D., Jahangiri, H.R., 2020. Data-driven technique for analyzing the injector efficiency in a waterflooding operation. Simulation 96, 701–710. https://doi.org/10.1177/0037549720923386.

Shakeel, M., Samanova, A., Pourafshary, P., Hashmet, M.R., 2021a. Capillary desaturation tendency of hybrid engineered water-based chemical enhanced oil recovery methods. Energies 14. https://doi.org/10.3390/en14144368.

Shakeel, M., Samanova, A., Pourafshary, P., Hashmet, M.R., 2021b. Experimental analysis of oil displacement by hybrid engineered water/chemical EOR approach in carbonates. J. Petrol. Sci. Eng., 109297 https://doi.org/10.1016/j.petrol.2021.109297.

Surajudeen, S., Yahya, N., Soleimani, H., Musa, A.A., Afeez, Y., Rostami, A., 2019. Effect OF adsorption ON saturated sandstone within electric double layer ON solid/liquid inter-phase. Petroleum & Coal 61.

Tang, G.-Q., Morrow, N.R., 1999. Influence of brine composition and fines migration on crude oil/brine/rock interactions and oil recovery. J. Petrol. Sci. Eng. 24, 99–111. https://doi.org/10.1016/S0920-4105(99)00034-0.

Vledder, P., Gonzalez, I.E., Carrera Fonseca, J.C., Wells, T., Ligthelm, D.J., 2010. Low salinity water flooding: proof of wettability alteration on A field wide scale. In: Paper Presented at the SPE Improved Oil Recovery Symposium, Tulsa, Oklahoma, USA, 2010/1/1/. https://doi.org/10.2118/129564-MS.

Yousef, A.A., Gentil, P.H., Jensen, J.L., Lake, L.W., 2006. A capacitance model to infer interwell connectivity from production and injection rate fluctuations. SPE-192289-PA 9, 630–646. https://doi.org/10.2118/95322-PA.

Yousefi, S.H., Rashidi, F., Sharifi, M., Soroush, M., 2019. Prediction of immiscible gas flooding performance: a modified capacitance–resistance model and sensitivity analysis. Petrol. Sci. 16, 1086–1104. https://doi.org/10.1007/s12182-019-0342-6.

Zhao, H., Ning, Z., Kang, Q., Chen, L., Zhao, T., 2017. Relative permeability of two immiscible fluids flowing through porous media determined by lattice Boltzmann method. Int. Commun. Heat Mass Tran. 85, 53–61. https://doi.org/10.1016/j.icheatmasstransfer.2017.04.020.

Zhao, J., Kang, Q., Yao, J., Viswanathan, H., Pawar, R., Zhang, L., Sun, H., 2018. The effect of wettability heterogeneity on relative permeability of two-phase flow in porous media: a lattice Boltzmann study. Water Resour. Res. 54, 1295–1311. https://doi.org/10.1002/2017WR021443.

Zivar, D., Pourafshary, P., Moradpour, N., 2021. Capillary desaturation curve: does low salinity surfactant flooding significantly reduce the residual oil saturation? Journal of Petroleum Exploration and Production 11, 783–794. https://doi.org/10.1007/s13202-020-01074-1.